The effect of species on lacustrine $\delta^{18}O_{diatom}$ and its implication for palaeoenvironmental reconstructions

Hannah L. Bailey[1*], Andrew C.G. Henderson[1], Hilary J. Sloane[2], Andrea Snelling[2], Melanie J. Leng[3,2] and Darrell S. Kaufman [4]

1. School of Geography Politics & Sociology, Newcastle University, Newcastle upon Tyne, NE1 7RU, UK.
2. NERC Isotope Geosciences Laboratory, British Geological Survey, Nottingham, Keyworth, NG12 5GG, UK.
3. Centre for Environmental Geochemistry, School of Geography, University of Nottingham, Nottingham, NG7 2RD, UK.
4. School of Earth Sciences and Environmental Sustainability, Northern Arizona University, Flagstaff, AZ 86011, USA.

[*]Corresponding Author: h.l.bailey@ncl.ac.uk

Abstract

The oxygen isotope composition of diatom silica ($\delta^{18}O_{diatom}$) is increasingly being used to reconstruct climate from marine and lacustrine sedimentary archives. Though diatoms are assumed to precipitate their frustule in isotopic equilibrium with their surrounding water, it is unclear whether internal processes of a given species affect the fractionation of oxygen between the water and the diatom. We present $\delta^{18}O_{diatom}$ data from two diatom size fractions (3-38 μm and >38 μm) characterized by different species in a sediment core from Heart Lake, Alaska. Differences in $\delta^{18}O_{diatom}$ between the two size fractions varies from 0 - 1.2 ‰, with a mean offset of 0.01 ‰ (n = 20). Fourier transform infrared (FTIR) spectroscopy confirms our samples consist of pure biogenic silica (SiO_2) and $\delta^{18}O_{diatom}$ trends are not driven by contamination. The maximum offset is outside the range of error, but the mean is within analytical error of the technique (±1.06 ‰), demonstrating no discernible species-dependent fractionation in $\delta^{18}O_{diatom}$. We conclude lacustrine $\delta^{18}O_{diatom}$ measurements offer a reliable and valuable method for reconstructing $\delta^{18}O_{water}$. Considering the presence of small offsets in our two records, we advise interpreting shifts in $\delta^{18}O_{diatom}$ only where the magnitude of change is greater than the combined analytical error.

Keywords: oxygen isotopes; diatom; lake; fractionation; palaeoclimate

Introduction

Diatoms are microscopic, unicellular algae with an external shell (frustule) composed of biogenic silica (opal, $SiO_2.nH_2O$) (Round *et al*. 2007). Distinct diatom communities exist due to variable ecological tolerances and optima (e.g. Moser *et al*. 1996; Battarbee *et al*. 2001) making them sensitive indicators of environmental change. Their siliceous frustules can be preserved over long timescales and are generally identifiable to the species level, enabling the reconstruction of past environments well beyond the instrumental record. The silica frustule comprises two layers: a tetrahedrally bonded silica layer (-Si-O-Si) which incorporates oxygen from the surrounding water during formation, and an outer hydrous layer (-Si-OH) which continues to exchange oxygen with the surrounding water following frustule formation (Leng and Swann, 2010). By isolating and extracting oxygen from the internal silica, the isotopic composition of the diatom ($\delta^{18}O_{diatom}$) can be determined and used to reconstruct past changes in climate (Leng and Barker, 2006).

The $\delta^{18}O_{diatom}$ value of a diatom frustule depends on the ambient water temperature and isotopic composition of the water ($\delta^{18}O_{water}$) in which the diatom grows (Labeyrie, 1974; Juillet-Leclerc and Labeyrie, 1987). By assuming $\delta^{18}O_{diatom}$ fractionates in isotopic equilibrium with this surrounding water, stratigraphic shifts in $\delta^{18}O_{diatom}$ can be used to infer changes in climate over time. The aspect of climate captured by $\delta^{18}O_{diatom}$ largely depends on local hydrology, climate, water residence time and seasonality of diatom growth. Previous studies have interpreted lacustrine $\delta^{18}O_{diatom}$ records to reflect changes in the precipitation/evaporation balance (P/E) (Rioual *et al*. 2001; Lamb *et al*. 2005), shifts in moisture source and regime (Shemesh *et al*. 2001a, b; Rosqvist *et al*. 2004; Jones *et al*. 2004; Leng *et al*. 2005; Schiff *et al*. 2009), changes in the amount and seasonality of precipitation (Barker *et al*. 2001; Morley *et al*. 2005; Mackay *et al*. 2013), and, to some extent, changes in temperature (Juillet-Leclerc and Labeyrie, 1987; Shemesh *et al*. 1995; Brandriss *et al*. 1998; Moschen *et al*. 2005). The oxygen isotope composition of marine diatoms has also been used to reconstruct palaeoceanographic conditions, whereby $\delta^{18}O_{diatom}$ is interpreted to reflect changes in sea surface temperature and surface salinity (e.g. Shemesh *et al*. 1992; Sancetta *et al*. 1985), sea ice extent and melt-water events (e.g. Shemesh *et al*. 1995; Swann *et al*. 2013; Pike *et al*. 2013), as well as changes in climate-ocean dynamics and ocean productivity (e.g. Juillet-Leclerc

and Schrader, 1987; Swann *et al*. 2006; Romero *et al*. 2011). $\delta^{18}O_{diatom}$ is therefore increasingly being used as an indicator of palaeoclimate from both marine and terrestrial sedimentary archives (Leng and Barker, 2006; Swann and Leng, 2009).

Following the development of the technique in the 1970's and 1980's (Labeyrie, 1974; Labeyrie and Juillet, 1982), efforts over the last decade have significantly advanced our understanding of $\delta^{18}O_{diatom}$ fractionation, as well as addressed problematic issues of sample contamination and silica maturation (see Leng and Henderson, 2013 for a review). As diatoms are ubiquitous in most aquatic environments, $\delta^{18}O_{diatom}$ data are particularly valuable in the absence of other available proxies for isotopic analysis such as authigenic carbonates and carbonate-based microfossils (e.g. foraminifera, ostracods). Examples of such environments include oceans and lakes in high latitudes where carbonates are often limited or absent (e.g. Rosqvist *et al*., 1999, 2004; Hu and Shemesh, 2003; Schiff *et al.,* 2009; Jones *et al*., 2004; Swann *et al*., 2010).

Vital effects on $\delta^{18}O_{diatom}$ fractionation

Diatoms are generally assumed to precipitate their frustules in isotopic equilibrium with the surrounding water ($\delta^{18}O_{water}$), and any biological fractionation is presumed to be constant. Furthermore, there is a growing consensus that fractionation between $\delta^{18}O_{diatom}$ and $\delta^{18}O_{water}$ is in the order of *c.* –0.2‰/°C (e.g. Brandriss *et al*. 1998; Moschen *et al*. 2005; Dodd & Sharp, 2010) enabling changes in $\delta^{18}O_{diatom}$ to be quantified over time. However, the $\delta^{18}O_{diatom}$ composition of a diatom frustule often differs from that predicted by thermodynamics; an offset often referred to as a 'vital effect' (or disequilibrium effect) (Leng and Barker, 2006). Such vital effects are well documented and better understood in biogenic carbonates such as foraminifera in the marine environment (Shackleton *et al*. 1973; Erez, 1978), and ostracods in the lacustrine environment (Xia *et al*. 1997; Wetterich *et al*. 2008). In these instances, vital effects may even serve as a valuable palaeoenvironmental indicator, for example to reconstruct ocean thermal stratification (e.g. Fairbanks and Wiebe, 1980; Ravelo and Fairbanks, 1992; Mulitza *et al*. 1997) or vertical temperature gradients (Tedesco *et al*. 2007; Steph *et al*. 2009) due to the varying depths and temperatures occupied by different species. However, the $\delta^{18}O$ of foraminiferal calcite is not only controlled by the physical and chemical properties of the water column (e.g.

$\delta^{18}O_{water}$, temperature, depth), but also by 'species-specific' vital effects; internal processes such as calcification rate (Ortiz *et al*. 1996), symbiont photosynthesis (Spero and Lea, 1993) and respiration (Wolf-Gladrow *et al*. 1999) of a given species which are known to affect isotope fractionation. Some studies have also demonstrated offsets can be found between the $\delta^{18}O$ of ostracods valves at different stages of growth (e.g. juvenile vs. adult) (von Grafenstein *et al*. 1999; Keatings *et al*. 2002).

Similarly, $\delta^{18}O$ vital effects in diatoms could result from species-specific fractionation, with a varying fractionation factor due to species dependent $\delta^{18}O$ uptake in equilibrium conditions, or a shortage or excess supply in non-equilibrium conditions (Chapligin *et al*. 2012). The internal processes within the frustule could theoretically alter $\delta^{18}O_{diatom}$ relative to the isotopic signal of the surrounding water, by an amount that could vary from species to species. However, unlike biogenic carbonates, these effects are poorly understood and much harder to observe, their small size (2 – 200 μm) making it difficult to isolate individual diatom species for isotope analysis. Isotope measurements are typically made on samples containing many tens of different diatom species. The possibility different diatom species fractionate oxygen differently is therefore problematic, especially as the abundance of different species changes through time downcore, and it is not possible to analyse the same species in every sample. A number of studies have found no evidence for vital effects between individual diatom species (e.g. Sancetta *et al*. 1985; Schmidt *et al*. 2001; Moschen *et al*. 2005). When small (0.2 – 0.6‰) offsets have been observed between different species, they are usually within the range of analytical reproducibility (e.g. Shemesh *et al*. 1995; Brandriss *et al*. 1998). More recently, however, an offset of *c.* 3.0 - 3.5‰ was suggested for two size fractions of marine diatoms in the NW Pacific (Swann *et al*. 2007; 2008). A potential species-driven offset has considerable implications for the applicability of $\delta^{18}O_{diatom}$ as a palaeoclimatic proxy in the marine environment, particularly as this magnitude of variation equates to a 15 – 16°C temperature difference. In the NW Pacific, these offsets were attributed to size-related effects associated with larger diatoms (>75 μm) (Swann *et al*. 2007), although the results were largely inconclusive.

Similar to biogenic carbonates, the habitat in which a diatom grows (e.g. benthic vs. planktonic; water depth) may also affect its isotope composition. For example the $\delta^{18}O$ of lake water may become more negative with increasing depth if lighter isotopes are preferentially evaporated at the surface (e.g. von Grafenstein *et al*. 1999). In addition, water temperature decreases with depth and may also influence the oxygen isotope fractionation of diatom silica (Juillet-Leclerc and Labeyrie, 1987; Shemesh *et al*. 1992; Brandriss *et al*. 1998; Moschen *et al*. 2005), which must be considered when interpreting records of $\delta^{18}O_{diatom}$. Any offset between diatom species could also derive from the timing of the diatom bloom in the water column and whether the $\delta^{18}O_{diatom}$ signal captured has a seasonal component (e.g. spring vs. autumn; temperature and precipitation). The interpretation of $\delta^{18}O_{diatom}$ from any sedimentary record therefore requires an understanding of the external processes affecting $\delta^{18}O_{diatom}$ at a particular site, such as climate, water inflow and outflow, lake residence time and diatom ecology.

Here, we examine the issue of species-dependent vital effects in $\delta^{18}O_{diatom}$ using lacustrine sediment material from Heart Lake on Adak Island, part of the Aleutian Island chain in southwest Alaska. By analysing the $\delta^{18}O_{diatom}$ value of two size fractions containing different diatom species, we investigate whether species specific fractionation of oxygen is evident in a lacustrine environment.

Study Site

Heart Lake, located on Adak Island in the NW Pacific (51.87°N, 176.63°W; Fig.1), is a small (<0.25 km^2) freshwater, through-flow lake. Separating the Bering Sea to the north and the Pacific Ocean to the south, the island experiences a cool, wet and windy maritime climate (Rodionov *et al*. 2005). Mean precipitation in January and July is 150.4 mm and 71.6 mm, respectively (1942-1996) (NOAA, 2013). The mean annual $\delta^{18}O$ of precipitation ($\delta^{18}O_{precip}$) is –8.80‰, varying slightly between January (–9.41‰) and July (–8.93‰) (IAEA, 2013). The correlation between $\delta^{18}O$ and $\delta^{2}H$ of available precipitation data from Adak (1962-1973) (IAEA, 2013) defines a local meteoric water line (LMWL) where $\delta^{2}H = 6.86\ \delta^{18}O - 3.26$ (Fig.2). The $\delta^{18}O$ of surface lake water samples collected in summer 2009 and 2010 are –9.75‰ and –9.24‰, and are similar to modern-day $\delta^{18}O_{precip}$ values. Therefore, evaporation of

surface waters has very little influence on the $\delta^{18}O$ of the lake and suggests that the $\delta^{18}O$ of Heart Lake reflects $\delta^{18}O_{precip}$ (rain and snowfall) received by the lake.

Methodology

Sample Material

A 5.5 m-long sediment core (AS-10-1D) was recovered from Heart Lake in July 2010. A GPS-enabled sonar depth recorder guided bathymetric profiling, and the core site was selected adjacent to the deepest part of the basin at 7.6 m-depth. The core was recovered using a percussion corer operated from a floating platform. The core was split, photographed and described (Kraweic, 2013), with 20 samples taken downcore for $\delta^{18}O_{diatom}$ and diatom species analysis. The samples range in age from 8.0 to 1.0k cal a BP based on a best-fit age-depth model constructed using AMS ^{14}C ages and correlated tephra ages from nearby Andrew Lake (Krawiec *et al*. 2013).

Sample Preparation

Samples for $\delta^{18}O_{diatom}$ were prepared using a stepwise process of chemical digestion, differential settling, sieving and heavy liquid separation based on Morley *et al*. (2004). Sediment samples were treated with 30% H_2O_2 at 90°C until reactions ceased (to remove organic material), before using 5% HCl to eliminate any carbonates. Following differential settling, all samples were centrifuged in sodium polytungstate ($3Na_2WO_4 9WO_3.H_2O$) (SPT) heavy liquid at 2500 rpm for 20 minutes, resulting in the separation and suspension of diatoms from the heavier detrital residue. This process was repeated three times using specific gravities of 2.50, 2.30 and 2.25 g ml^{-1}. After the final SPT separation, samples were washed five times at 1500 rpm for 5 minutes to remove any remaining SPT. Purified diatom samples were then sieved at 38 µm and 3 µm, resulting in two size fractions of 3–38 µm and >38 µm for $\delta^{18}O_{diatom}$ analysis. The < 3 µm fraction was discarded as it was too small (~1 mg) to be analysed. The remaining fractions (3-38 and >38µm) of the sample were then treated with an additional stage of 30% H_2O_2 at 70°C for one week and centrifuge washed to ensure no traces of organic matter remained.

Sub-samples of the purified diatom material were retained and mounted on cover slips using Naphrax®. The samples were visually inspected for contamination before

diatom assemblage analysis using light microscopy (300 frustules per sample). Standard diatom preparation and analysis (Battarbee *et al*. 2001) was also performed on the unprocessed lake sediment to identify the diatom assemblages species present and determine whether any species were lost during preparation for diatom isotope analysis.

Contamination Assessment

Fourier transform infrared spectroscopy (FTIR) was used as a rapid, non-destructive means to assess the chemical composition of biogenic silica within our samples (Leng *et al*. 2009), and ultimately sample purity (see Swann and Patwardham, 2011). Sixteen purified diatom samples, together with the within-run laboratory diatom standard (BFC_{mod}) were analysed using FTIR (Fig. 3). FTIR produces energy absorption spectra of a sample over a range of wavelengths. Individual absorption peaks correspond to specific chemical bonds and compounds, with pure silica displaying peaks in two distinct regions at >2500 cm^{-1} (hydroxyl) and <1300 cm^{-1} (silica) (Fidalgo and Ilharco, 2001; Patwardhan *et al*. 2006; Swann and Patwardhan, 2011). FTIR analyses of all purified diatom isotope samples indicate peaks corresponding to the BFC_{mod} standard, known to represent clean, fossillised diatomite (Fig.3). Spectral deviation from the standard would indicate additional compounds within the sample and contamination by non-diatom components (Swann and Patwardhan, 2011). Peaks centered at ~450 cm^{-1}, ~800 cm^{-1} and ~1100 cm^{-1} indicate pure silica and suggest that the samples comprise purely diatoms. Additionally, scanning electron microscope (SEM) imaging was used to check sample purity prior to oxygen isotope analysis (Fig.4).

Oxygen Isotope Analysis

Purified diatom samples were analysed for $\delta^{18}O_{diatom}$ at the NERC Isotope Geosciences Laboratory (UK) using a step-wise fluorination method outlined in Leng and Barker (2006). The outer hydrous layer of the diatom, known to freely exchange isotopically with water (e.g. Juillet-Leclerc and Labeyrie, 1987), was removed in a pre-fluorination stage using a BrF_5 reagent at low temperature. This was followed by a full reaction at high temperature to liberate oxygen that was converted to CO_2 (Clayton and Mayeda, 1963) and measured for $\delta^{18}O_{diatom}$ using a MAT 253 dual-inlet

mass spectrometer. All $\delta^{18}O$ values were converted to the VSMOW scale using the within-run laboratory standard BFC_{mod}, and are reported here in per mil (‰).

Results

Diatom Assemblages

Diatom frustules are well preserved in all 60 samples as indicated by SEM images that show no evidence of valve dissolution (Fig. 4). The smaller size fraction (3-38 μm) is taxonomically diverse, with 120 diatom species identified. The flora is dominated by seven species (*Psammothidium levanderi, Rossithidium pusillum, Cyclotella rossii, Pseudostaurosira brevistriata, Staurosira construens, Stauroforma exiguiformis and Staurosirella pinnata*) with a combined relative abundance of 76 % across all samples (Fig. 4b). Subtle shifts in species assemblages are evident among the samples, with the most notable transition at *c*. 320 cm depth, when the abundance of *P. levanderi* and *C. rossii* decline markedly and the abundance of the small *Staurosira/Staurosirella* species increasingly dominate. In the larger size fraction (>38), 28 different diatom species were identified. The assemblages are dominated by six species (*Didymosphenia geminata, Surirella robusta*, *Surirella splendida Pinnularia turnerae*, *Rhopalodia gibba* and *Campylodiscus hibernicus*), with a combined relative abundance of 85% across all samples (Fig.4a). The diatom assemblage in this larger fraction is distinctly different from that of the smaller size fraction; they are not merely larger specimens of the same species. The transition at ~320 cm depth is also evident in the larger size fraction, with a marked increase in *D.geminata*, *P.turnerae* and *R.gibba*, which replace *C.hibernicus* and *Surirella* species. The unprocessed bulk sediment samples are composed of the same diatom assemblages found in both the purified $\delta^{18}O_{diatom}$ size fractions (Fig.4c). Most notably however, the larger >38 μm diatoms only represent ~1% of the relative abundance across all bulk sediment samples.

$\delta^{18}O_{diatom}$ Values

The $\delta^{18}O_{diatom}$ values from Heart Lake range from +28.8‰ to +33.4‰ (Table 1; Fig. 5). Comparing the two size fractions, $\delta^{18}O_{diatom}$ values differ by 0 – 1.2‰ (r^2 = 0.75, *p* = <0.05), with a mean difference of –0.01‰. Duplicate analyses of $\delta^{18}O_{diatom}$ indicate an analytical reproducibility (1σ) of ± 0.19‰ for the smaller (3-38 μm) fraction, ± 0.49‰ for the larger (> 38 μm) fraction, and ±0.31‰ for the BFC_{mod} laboratory

diatom standard. All 20 pairs have $\delta^{18}O_{diatom}$ values within the combined analytical uncertainty of ± 1.06‰ (2σ) for the two size fractions. Neither fraction is consistently more isotopically positive or negative relative to the other, and the two values are similar down core, aside from two samples at 147.5 cm and 161.5 cm depth where they diverge.

The relationships between $\delta^{18}O_{diatom}$ and diatom assemblages were evaluated using principal components analysis (PCA) (Fig.5b, c) (ter Braak and Prentice, 1988). A PCA was applied to a correlation matrix based on the dominant diatom species in all 20 samples, in both size fractions. The stratigraphic changes are captured in the first and second PCA axes, which account for 49.9% and 29.9% of variance in the small size fraction (Fig.5b), and 55.3% and 17.0% in the large fraction (Fig. 5c).

Discussion

All 20 pairs of diatom size fractions have differences in $\delta^{18}O_{diatom}$ within the 2σ uncertainty range of this technique. Furthermore, the mean difference between the two data sets is close to zero (μ = –0.01‰) and indicates the two $\delta^{18}O_{diatom}$ records are not statistically different (Fig. 6).

The diatom assemblages from the two size fractions are composed of entirely different species, and the relative abundance of each species varies through time (Fig. 4). The main growing season of diatoms identified in Heart Lake occurs in spring following winter snow melt, when sediment and nutrient input to the lake is high and temperatures begin to increase. While some species such as *D. geminata* are known to reside in freshwaters all year round, the main bloom occurs in late spring and summer (Whitton *et al*. 2009). *C. hibernicus*, which is dominant in the lower section of the core, also blooms in both spring and autumn (Griffiths, 1923; Ramrath *et al*. 1999). Autumn diatom blooms are typically caused by the breakdown of summer stratification and entrainment of nutrients while there are still sufficient light levels for growth (Round *et al*. 2007). Temperatures in Heart Lake are consistently low year-round and the lake water is well mixed, meaning autumn blooms are unlikely to occur. As a result, both size fractions of the diatom sample capture the spring/summer $\delta^{18}O_{diatom}$ signal when their silica frustule is formed

(Moschen *et al*. 2005), and this rules out possible 'seasonal-effects' on $\delta^{18}O_{diatom}$ values.

Aside from the planktonic/tychoplanktonic species *C. rossii*, all of the dominant diatom species in Heart Lake are generally benthic and occupy the same habitat and pool of water ($\delta^{18}O_{water}$). Heart Lake is 7.6 m deep and is likely to be well mixed. Given the similarity between the $\delta^{18}O$ value of precipitation and lake water at Heart Lake, isotopic enrichment due to evaporation is insignificant. Any so-called water column effect is likely only applicable to deeper lakes than Heart Lake, or within the marine environment where there may be variations associated with different water masses. We can therefore assume all pairs of diatom fractions analysed for $\delta^{18}O_{diatom}$ formed their silica frustules under the same environmental conditions (i.e. depth, temperature, $\delta^{18}O_{water}$). Even though there are subtle differences between species habit, with some being solitary (*i.e. C. hibernicus*), some colonial (*i.e. D. geminata*), others motile (*i.e. C. rossii*), attached to substrata (*i.e. R. gibba*) or a combination of the above, these attributes appear insignificant given there is no discernible difference in $\delta^{18}O_{diatom.}$

Evidence of a size-related species effect on $\delta^{18}O_{diatom}$ has previously been documented in the marine environment, although these results are rather inconclusive. Swann *et al*. (2007) report more positive values of $\delta^{18}O_{diatom}$ in smaller diatoms compared to larger ones; but further research suggested the opposite (Swann *et al*. 2008). Diatom size is also inherently linked to growth rate, with most diatoms exhibiting a gradual reduction in size/growth with increasing maturity and successive cell division (Round *et al*. 2007). We cannot quantify the growth rate of specific diatoms within our sediment record, but we note in each size fraction the diameter of any given specie does not vary visibly (Fig. 4). While it would be incorrect to assume growth rates are consistent across all species, there is no evidence for a relationship between diatom size and the amount of fractionation in our samples, with no one size fraction consistently more positive or negative in $\delta^{18}O_{diatom}$ relative to the other (and within analytical error).

Visual inspection of all samples by light microscopy and SEM imaging revealed no obvious sign of contamination (e.g. SPT, minerals, tephra), which is further

confirmed by FTIR analysis. As the fluorination process will liberate oxygen from any oxygen-bearing mineral in the sample (Brewer *et al*. 2008), having ensured the diatoms are clean and free from contaminant, we consider the $\delta^{18}O_{diatom}$ data to be reliable.

Species-specific effects

In the large size fraction (>38μm), the diatom species *C.hibernicus* and *R.gibba* show the strongest correlation with downcore variation in $\delta^{18}O_{diatom}$, in positive and negative associations (i.e. with more positive $\delta^{18}O_{diatom}$, the abundance of *C.hibernicus* increases and the abundance of *R.gibba* decreases) (Fig. 5c). In the small (3-38 μm) diatom fraction, *C.rossii* and *S.construens* are most closely related with $\delta^{18}O_{diatom}$, in positive and negative associations (Fig. 5b). The remaining dominant diatom species, in both size fractions, appear unrelated to the $\delta^{18}O_{diatom}$ vector in the PCA, with several species being orthogonal to the $\delta^{18}O_{diatom}$ gradient (*D. geminata*, *S. splendida*, *P. turnerae*, *P. brevistriata*, *R. pusillum*). (Fig. 5b, c). Given only two different species drive ~50% of the variance in each size fraction, and there is no discernible difference in the $\delta^{18}O_{diatom}$ signal from these two fractions, we therefore find no evidence to suggest there is a species-driven effect controlling $\delta^{18}O_{diatom.}$ *C. hibernicus* disappears from Heart Lake after 254.5 cm, but there is no evidence of a concurrent shift in the $\delta^{18}O_{diatom}$ record at this time. The data therefore suggest stratigraphic shifts in diatom assemblages are ecological responses to climatic and environmental changes, as well as in the $\delta^{18}O_{diatom}$ record, rather than driving the isotopic signal thorough differences in species-specific fractionation. Determining the precise environmental and ecological factors driving species assemblages and changes to $\delta^{18}O_{diatom}$ is, however, beyond the scope of this paper. In this study, samples were initially analyzed downcore to represent different environmental conditions and assemblages to test for a possible species effects on oxygen isotopes in diatoms.

The diatom composition of the two size fractions analysed here represents different species assemblages and are considered independent of each other. If species-dependent vital effects were present, we would expect the $\delta^{18}O_{diatom}$ data for each size fraction to deviate and be consistently offset from one another. While the data do not establish whether diatoms precipitate their silica in isotopic equilibrium with

lake water, they demonstrate different species of diatoms fractionate oxygen isotopes at a similar magnitude.

Conclusions

$\delta^{18}O$ from diatom silica is generally presumed to precipitate in isotopic equilibrium with the surrounding water, however the presence of species-dependent vital effects on fractionation has, until now, been unclear. Our $\delta^{18}O_{diatom}$ data from Heart Lake reveal only small differences (0 - 1.2‰, n = 20) between two size fractions containing different diatom species assemblages. Given all differences are within the combined analytical error of the technique, it suggests there is no species or size-related effects controlling fractionation of $\delta^{18}O_{diatom}$ and bulk $\delta^{18}O_{diatom}$ samples are suitable for investigating palaeoenvironmental change at Heart Lake.

Diatom species analyses of both the raw sediment and the purified diatom samples reveal some diatom species were lost during preparation for diatom oxygen isotopes. However, considering these species account for < 1% of overall abundance across all samples, we conclude the purified samples analysed for $\delta^{18}O_{diatom}$ are representative of the species found within the raw sediment. It is therefore advised samples for $\delta^{18}O_{diatom}$ follow the same rigorous preparation and analytical procedures employed here.

We conclude $\delta^{18}O_{diatom}$ measurements from lacustrine diatom silica are a reliable and valuable method for reconstructing past $\delta^{18}O_{water}$. As diatoms are found in nearly all aquatic environments, $\delta^{18}O_{diatom}$ records offer an important source of information in regions devoid of other proxies available for isotopic analysis (e.g. carbonates), such as in the high latitude regions. Considering the presence of small offsets in our two records, we advise interpreting shifts in $\delta^{18}O_{diatom}$ only where the magnitude of change is greater than the combined analytical error for those samples.

Acknowledgements

The research was supported by a NERC CASE studentship award to HLB (NE/I528350/1) and a NERC Isotope Geosciences Facilities grant to ACGH (IP/1202/1110). Recovery of water samples, sediment core material and the

development of the age model was supported by a NSF grant to DSK (EAR 0823522). The authors thank Anne Krawiec and David Vaillencourt at NAU for field assistance and for use of their age model.

References

Barker, P.A., Street-Perrott, F.A., Leng, M.J., Greenwood, P.B., Swain, D.L., Perrott, R.A., Telford, J. and Ficken, K.J. (2001) A 14 ka oxygen isotope record from diatom silica in two alpine tarns on Mt. Kenya. *Science* **292**, 2307-2310.

Battarbee, R.W., Carvalho, L. and Juggins, S. (2001) Chapter 8. Diatoms in J.P. Smol, H.J.B. Birks and W.M. Last (eds.) *Tracking Environmental Change Using Lake Sediments. Volume 3: Terrestrial, Algal, and Siliceous Indicators.* Kluwer Academic Publishers, Dordrecht, The Netherlands.

Brandriss, M.E., O'Neil, J.R., Edlund, M.B. and Stoermer, E.F. (1998) Oxygen isotope fractionation between diatomaceous silica and water. *Geochemica et Cosmochimica Acta* **62**, 1119-1125.

Brewer, T.S., Leng, M.J., Mackay, A.W., Lamb, A.L., Tyler, J.J. and Marsh, N.G. (2008) Unraveling contamination signals in biogenic silica oxygen isotope composition: the role of major and trace element geochemistry. *Journal of Quaternary Science* **23**, 321-330.

Chapligin, B., Meyer, H., Bryan, A., Snyder, J. and Kemnitz, H. (2012) Assessment of purification and contamination correction methods for analysing the oxygen isotope composition from biogenic silica. *Chemical Geology* **300-301**, 185-199.

Clayton, R.N. and Mayeda, T.K. (1963) The use of bromine pentafluoride in the extraction of oxygen from oxide and silicates for isotopic analysis. *Geochimica et Cosmochimica Acta* **27**, 43-52.

Cole, J.E., Rind, D., Webb, R.S., Jouzel, J. and Healy, R. (1999) Climatic controls on interannual variability of precipitation delta O-18: simulated influence of temperature, precipitation amount, and vapor source region. *Journal of Geophysical Research: Atmospheres* **104**, 14223– 14235.

Erez, J. (1978) Vital effect on stable-isotope composition seen in foraminifera and coral skeletons. *Nature* **273**, 199–202.

Fairbanks, R.G. and Wiebe, P.H. (1980) Foraminifera and Chlorophyll Maximum: Vertical Distribution, Seasonal Succession, and Paleoceanographic Significance. *Science* **209**, 1524-1526.

Fidalgo, A. and Ilharco, L.M. (2001) The defect structure of sol-gel-derived silica/polytetrahydrofuran hybrid films by FTIR. *Journal of Non-Crystalline Solids* **283**, 144-54.

Griffiths, B.M. (1923) The phytoplankton of bodies of fresh water, and the factors determining its occurrence and composition. *Journal of Ecology* **11**, 184-213.

Hu, F.S. and Shemesh, A. (2003) A biogenic-silica $\delta^{18}O$ record of climatic change during the last glacial-interglacial transition in southwestern Alaska. *Quaternary Research* **59**, 379 – 385.

IAEA (2013) Global network of isotopes in precipitation. The GNIP database. Retrieved 14 January 2013 from http://www-naweb.iaea.org.

Jones, V.J., Leng, M.J., Solovieva, N., Sloane, H.J. and Tarasov, P. (2004) Holocene climate of the Kola Peninsula; evidence from the oxygen isotope record of diatom silica. *Quaternary Science Reviews* **23**, 833 – 839.

Juillet-Leclerc, A. and Labeyrie, L. (1987) Temperature dependence of the oxygen isotopic fractionation between diatom silica and water. *Earth and Planetary Science Letters* **84**, 69-74.

Juillet-Leclerc, A. and Schrader, H. (1987) Variations of upwelling intensity recorded in varved sediment from the Gulf of California during the past 3,000 years. *Nature* **329**, 146–149.

Keatings, J.W., Heaton, T.H.E. and Holmes, J.A. (2002) Carbon and oxygen isotope fractionation in non-marine ostracods: results from a 'natural culture' environment. *Geochimica et Cosmochimica Acta* **66**, 1701-1711.

Krawiec, A.C.L. (2013) Holocene Tephrochronology and Storminess Inferred from Two Lakes on Adak Island, Alaska. M.S. Thesis. Northern Arizona University, 107 p.

Krawiec, A.C.L., Kaufman, D.S. and Vaillencourt, D.A. (2013) Age models and tephrostratigraphy from two lakes on Adak Island, Alaska. *Quaternary Geochronology* **18**, 41-53.

Labeyrie, L.D. (1974) New approach to surface seawater palaeotemperatures using $^{18}O/^{16}O$ ratios in silica of diatom frustules. *Nature* **248**, 40-42.

Labeyrie, L.D. and Juillet, A. (1982) Oxygen isotope exchangeability of diatom valve silica; interpretations and consequences for paleoclimatic studies. *Geochimica et Cosmochimica Acta* **46**, 967-975.

Lamb, A.L., Brewer, T.S., Leng, M.J., Sloane, H.J. and Lamb, H.F. (2005) A geochemical method for removing the effect of tephra on lake diatom oxygen isotope records. *Journal of Paleolimnology* **37**, 499-516.

Leng, M.J. and Barker, P.A. (2006) A review of the oxygen isotope composition of lacustrine diatom silica for palaeoclimate reconstruction. *Earth Science Reviews* **75**, 5 – 27.

Leng, M.J. and Henderson, A.C.G. (2013) Recent advances in isotopes as palaeolimnological proxies. *Journal of Paleolimnology* **49**, 481-496.

Leng, M.J. and Swann, G.E.A. (2010) *Stable Isotopes in Diatom Silica.* In: J.P. Smol and E.F. Stoermer. The Diatoms: applications for the Environmental and Earth Sciences, Cambridge Press, pp 667.

Leng, M.J., Metcalfe, S.E. and Davies, S.J. (2005) Investigating late Holocene climate variability in central Mexico using carbon isotope ratios in organic materials and oxygen isotope ratios from diatom silica within lacustrine sediments. *Journal of Palaeolimnology* **34**, 413– 431.

Leng, M.J., Swann, G.E.A., Hodson, M.J., Tyler, J.J., Patwardhan, S.V. and Sloane, H.J. (2009) The potential use of silicon isotope composition of biogenic silica as a proxy for environmental change. *Silicon* **1**, 65-77.

Mackay, A.W., Swann, G.E.A., Fagel, N., Fietz, S., Leng, M.J., Morley, D., Rioual, P. and Tarasov, P. (2013) Hydrological instability during the Last Interglacial in central Asia: a new diatom oxygen isotope record from Lake Baikal. *Quaternary Science Reviews* **66**, 45-54.

Morley, D.W., Leng, M.J., Mackay, A.W., Sloane, H.J., Rioual, P. and Battarbee, R.W. (2004) Cleaning of lake sediment samples for diatom oxygen isotope analysis. *Journal of Paleolimnology* **31**, 391-401.

Morley, D.W., Leng, M.J., Mackay, A.W. and Sloane, H.J. (2005) Late glacial and Holocene environmental change in the Lake Baikal region documented by oxygen isotopes from diatom silica. *Global and Planetary Change* **46**, 221-233.

Moschen, R., Lücke, A. and Schleser, G. (2005) Sensitivity of biogenic silica oxygen isotopes to changes in surface water temperature and palaeoclimatology. *Geophysical Research Letters* **32**, L07708, doi: 10.1029/2004GL022167.

Moser, K.A., MacDonald, G.M. and Smol, J.P. (1996) Applications of freshwater diatoms to geographical research. *Progress in Physical Geography* **20**, 21-52.

Mulitza, S., Dürkoop, A., Hale, W., Wefer, G. and Niebler, H.S. (1997) Planktonic foraminifera as recorders of past surface-water stratification. *Geology* **25**, 335-338.

NOAA (2013) *National Oceanic and Atmospheric Administration*. National Climatic Data Centre. Retrieved 16 January 2013 from http://www.ncdc.noaa.gov/land-based-station-data.

Ortiz, J.D., Mix, A.C., Rugh, W., Watkins, J.M. and Collier, R.W. (1996) Deep-dwelling planktonic foraminifera of the northeastern Pacific Ocean reveal environmental control of oxygen and carbon isotopic disequilibria. *Geochimica et Cosmochimica Acta* **60**, 4509-4523.

Patwardhan, S.V., Maheshwari, R., Mukherjee, N., Kiick, K.L. and Clarson, S.J. (2006) Conformation and Assembly of Polypoptide Scaffolds in Templating the Synthesis of Silica: an example of a polylysine macromolecular “switch”. *Biomacromolecules* **7**, 491-497.

Pike, J., Swann, G.E.A., Leng, M.J. and Snelling, A.M. (2013) Glacial discharge along the west Antarctic Peninsula during the Holocene. *Nature Geoscience* **6**, 199-202.

Ramrath, A., Nowaczyk, N.R. and Negendank, J.F.W. (1999) Sedimentological evidence for environmental changes since 34,000 years BP from Lago di Mezzano, central Italy. *Journal of Paleolimnology* **21**, 423-435.

Ravelo, C.A. and Fairbanks, R.G. (1992) Reconstructing the photic zone temperature range using $\delta^{18}O$ measured on multiple species of planktonic foraminifera. *Paleoceanography* **7**, 815-832.

Rioual, P., Andrieu-Ponel, V., Rietti-Shati, M., Battarbee, R.W., de Beaulieu, L-J., Cheddadi, R., Reille, M., Svobodova, H. and Shemesh, A. (2001) High-resolution record of climate stability in France during the last interglacial period. *Nature* **413**, 293-296.

Rodionov, S.N., Overland, J.E. and Bond, N.A. (2005) Spatial and temporal variability of the Aleutian climate. *Fisheries Oceanography* **14**, 3-21.

Romero, O.E., Swann, G.E.A., Hodell, D.A., Helmke, P., Rey, D. and Rubio, B. (2011) A highly productive Subarctic Atlantic during the Last Interglacial and the role of diatoms. *Geology* **39**, 1015-1018.

Rosqvist, G.C., Rietti-Shati, M. and Shemesh, A. (1999) Late glacial to middle Holocene climatic record of lacustrine biogenic silica oxygen isotopes from a Southern Ocean island. *Geology* **27**, 967 – 970.

Rosqvist, G.C., Jonsson, C., Yam, R., Karlen, W. and Shemesh, A. (2004) Diatom oxygen isotopes in pro-glacial lake sediments from northern Sweden: a 5000 year record of atmospheric circulation. *Quaternary Science Reviews* **23**, 851 – 859.

Round, F.E., Crawford, R.W. and Mann, D.G. (2007) *The Diatoms: Biology and Morphology of the Genera*. Cambridge University Press: Cambridge.

Sancetta, C., Heusser, L., Labeyrie, L., Sathy Naidu, A. and Robinson, S.W. (1985) Wisconsin-Holocene paleoenvironment of the Bering Sea: evidence from diatoms, pollen, oxygen isotopes and clay minerals. *Marine Geology* **62**, 55-68.

Schiff, C.J., Kaufman, D.S., Wolfe, A.P., Dodd, J. and Sharp, Z. (2009) Late Holocene storm-trajectory changes inferred from the oxygen isotope composition of lake diatoms, south Alaska. *Journal of Paleolimnology* **41**, 189 – 208.

Schmidt, M., Botz, R., Rickert D., Bohrmann, G., Hall, S.R. and Mann, S. (2001) Oxygen isotope of marine diatoms and relations to opal-A maturation. *Geochemica et Cosmochimica Acta* **65**, 201-211.

Shackleton, N.J., Wiseman, J.D.H. and Buckley, H.A. (1973) Non-equilibrium isotopic fractionation between seawater and planktonic foraminiferal tests. *Nature* **242**, 177–179.

Shemesh, A., Charles, C.D. and Fairbanks, R.G. (1992) Oxygen isotopes in biogenic silica: global changes in ocean temperature and isotopic composition. *Science* **256**, 1434–1436.

Shemesh, A., Burckle, L.H. and Hays, J.D. (1995) Late Pleistocene oxygen isotope records of biogenic silica from the Atlantic sector of the Southern Ocean. *Paleoceanography* **10**, 179-196.

Shemesh, A., Rietti-Shati, M., Rioual, P., Battarbee, R.W., de Beaulieu, J-L., Reille, M., Andrieu, V. and Svobodova, H. (2001a) An oxygen isotope record of lacustrine opal from a European Maar indicates climatic stability during the last interglacial. *Geophysical Research Letters* **28**, 2305-2308.

Shemesh, A., Rosqvist, G., Rietti-Shati, M., Rubensdotter, L., Bigler, C., Yam, R. and Karlen, W. (2001b) Holocene climatic change in Swedish Lapland inferred from an oxygen-isotope record of lacustrine biogenic silica. *Holocene* **11**, 447–454.

Spero, H.J. and Lea, D.W. (1993) Intraspecific stable isotope variability in the planktonic foraminifera Globigerinoides sacculifer: results from laboratory experiments. *Marine Micropaleontology* **22**, 221–234.

Steph, S., Regenberg, M., Tiedemann, R., Mulitza, S. and Nürnberg, D. (2009) Stable isotopes of planktonic foraminifera from tropical Atlantic/Caribbean core-tops: Implications for reconstructing upper ocean stratification. *Marine Micropaleontology* **71**, 1-19.

Swann, G.E.A. and Leng, M.J. (2009) A review of diatom $\delta^{18}O$ in palaeoceanography. *Quaternary Science Reviews* **28**, 384 – 398.

Swann, G.E.A. and Patwardhan, S.V. (2011) Application of Fourier Transform Infrared Spectroscopy (FTIR) for assessing biogenic silica sample purity in geochemical analyses and palaeoenvironmental research. *Climate of the Past* **7**, 65-74.

Swann, G. E. A.,Maslin, M.A., Leng, M.J., Sloane, H.J. and Haug, G.H. (2006) Diatom $\delta^{18}O$ evidence for the development of the modern halocline system in the subarctic northwest Pacific at the onset of major Northern Hemisphere glaciations. *Paleoceanography* **21**, PA1009, doi:10.1029/2005PA001147.

Swann, G.E.A., Leng, M.J., Sloane, H.J., Maslin, M.A. and Onodera, J. (2007) Diatom oxygen isotopes: Evidence of a species effect in the sediment record. *Geochemistry Geophysics Geosystems* **8**, Q06012.

Swann, G.E.A., Leng, M.J., Sloane, H.J. and Maslin, M.A. (2008) Isotope offsets in marine diatoms $\delta^{18}O$ over the last 200 ka. *Journal of Quaternary Science* **23**, 389-400.

Swann, G.E.A., Leng, M.J., Juschus, O., Melles, M., Brigham-Grette, J. and Sloane, H.J. (2010) A combined oxygen and silicon diatom isotope record of Late Quaternary change in Lake El'gygytgyn, North East Siberia. *Quaternary Science Reviews* **29**, 774 – 786.

Swann, G.E.A., Pike, J., Snelling, A.M., Leng, M.J. and Williams, M.C. (2013) Seasonally resolved diatom $\delta^{18}O$ records from the west Antarctic Peninsula over the last degalciation. *Earth and Planetary Science Letters* **364**, 12-23.

Tang, E.P.Y. (1995) The allometry of algal growth rates. *Journal of Plankton Research* **17**, 1325-1335.

Tedesco, K.A., Thunell, R., Astor, Y. and Muller-Karger, F. (2007) The oxygen isotope composition of planktonic foraminifera from the Cariaco Basin, Venezuela: Seasonal and interannual variations. *Marine Micropaleontology* **62**, 180-193.

ter Braak, C.J.F. and Prentice, I.C. (1988) A theory of gradient analysis. *Advances in Ecological Research* **18**, 271-317.

von Grafenstein, U., Erlenrkeuser, H. and Trimborn, P. (1999) Oxygen and carbon isotopes in modern freshwater ostracods valves: assessing vital offsets and autecological effects of interest for palaeoclimate studies. *Palaeogeography, Palaeoclimatology, Palaeoecology* **148**, 133-152.

Wetterich, S., Schirrmeister, L., Meyer, H., Viehberg, F. and Mackensen, A. (2008) Arctic freshwater ostracods from modern periglacial environments in the Lena River Delta (Siberian Arctic, Russia): geochemical applications for palaeoenvironmental reconstructions. *Journal of Paleolimnology* **39**, 427–449.

Whitton, B.A., Ellwood, N.T. and Kawecka, B. (2009) Biology of the freshwater diatom Didymosphenia: a review. *Hydrobiologia* **630**, 1-37.

Wolf-Gladrow, D. A., Riebesell, U., Burkhardt, S. and Bijma, J. (1999) Direct effects of CO_2 concentration on growth and isotopic composition of marine plankton. *Tellus B* **51**, 461–476.

Xia, J., Ito, E. and Engstrom, D.R. (1997) Geochemistry of ostracod calcite: Part 1. An experimental determination of oxygen isotope fractionation. *Geochimica et Cosmochimica Acta* **61**, 377–382.

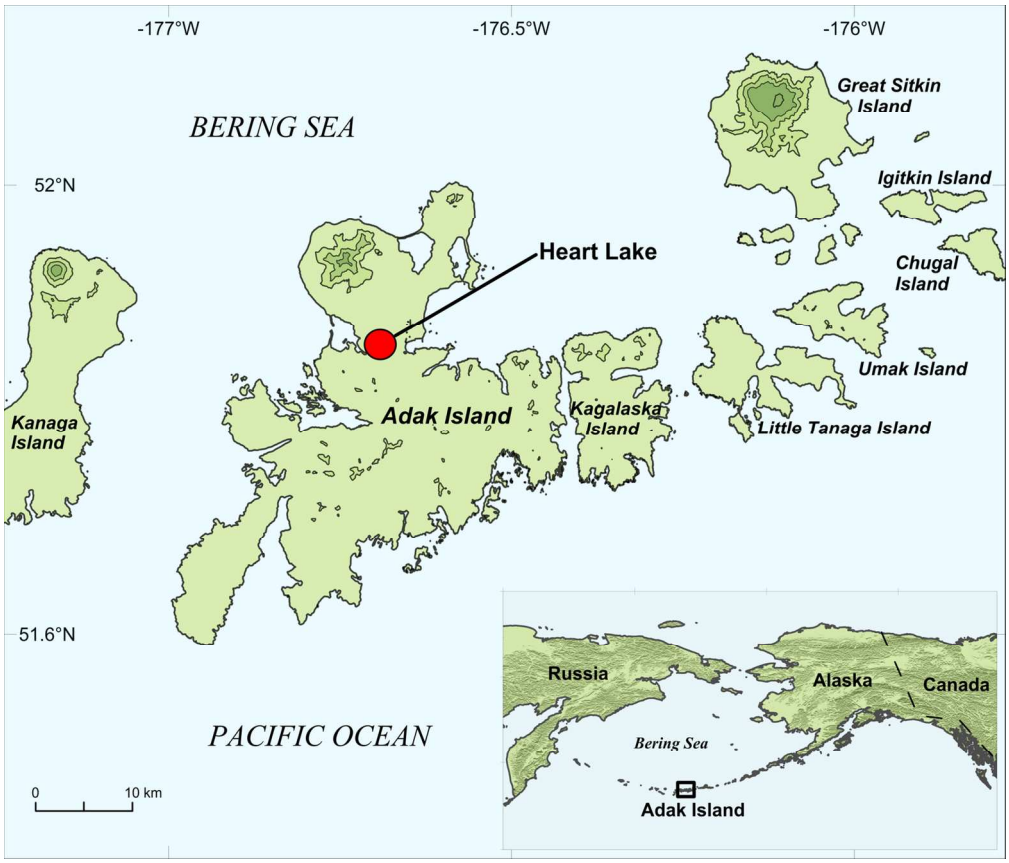

Figure 1. Location of Heart Lake on Adak Island, SW Alaska
71x60mm (600 x 600 DPI)

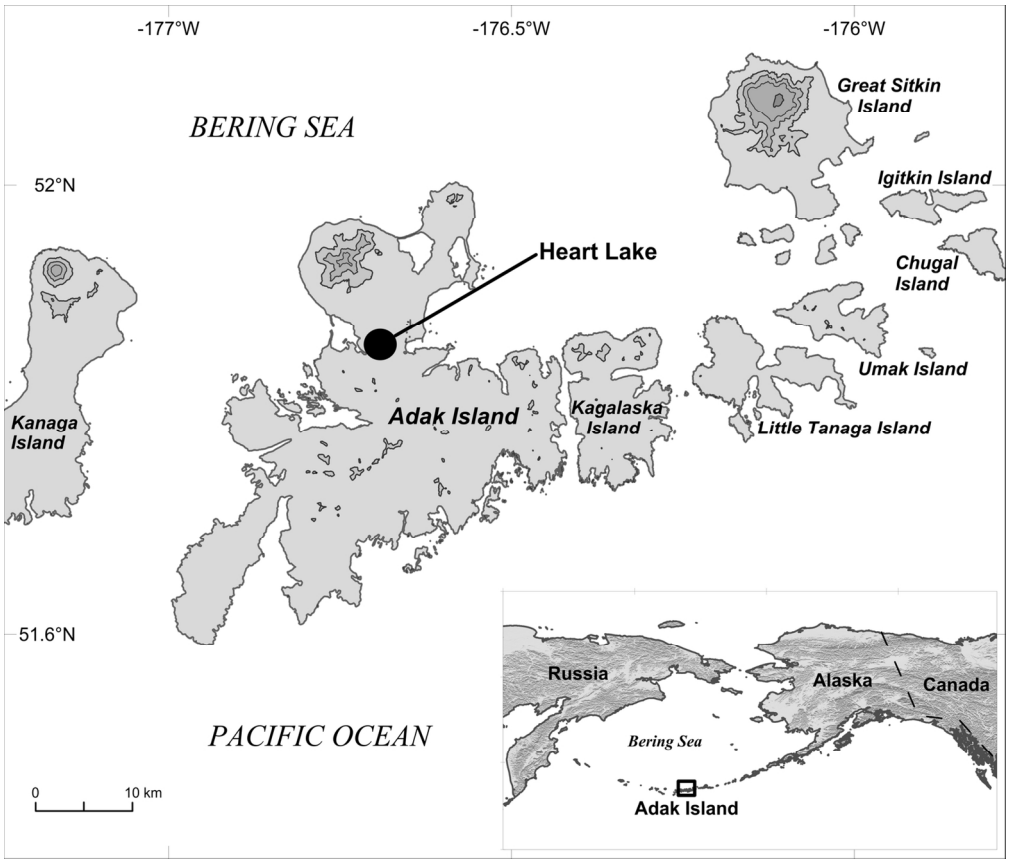

Figure 1. Location of Heart Lake on Adak Island, SW Alaska
71x60mm (600 x 600 DPI)

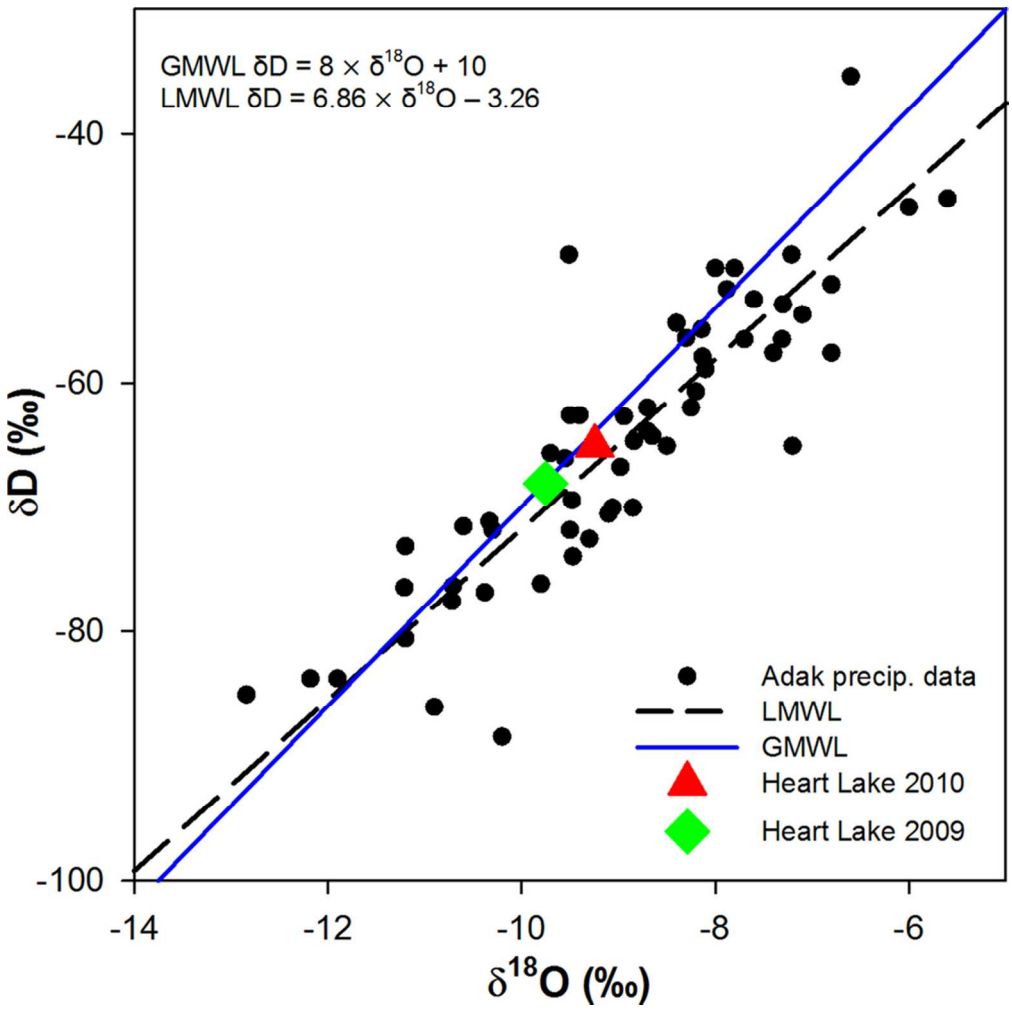

Figure 2. Heart Lake surface water $\delta^{18}O$ (2009 and 2010) on the local meteoric water line (LWML) and the global meteoric water line (GMWL). LMWL data are derived from Adak precipitation samples collected by the Global Network of Isotopes in Precipitation (GNIP)
83x83mm (300 x 300 DPI)

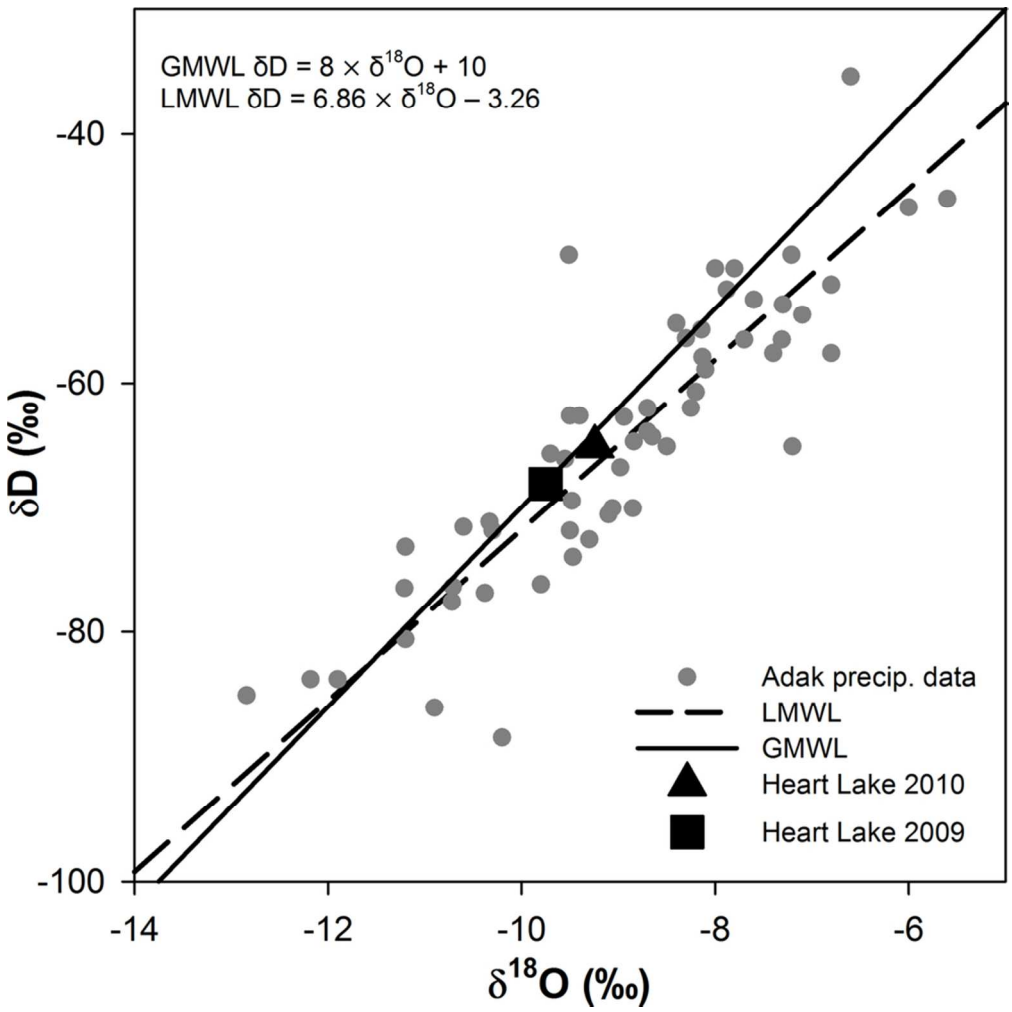

Figure 2. Heart Lake surface water $\delta^{18}O$ (2009 and 2010) on the local meteoric water line (LWML) and the global meteoric water line (GMWL). LMWL data are derived from Adak precipitation samples collected by the Global Network of Isotopes in Precipitation (GNIP)
83x83mm (300 x 300 DPI)

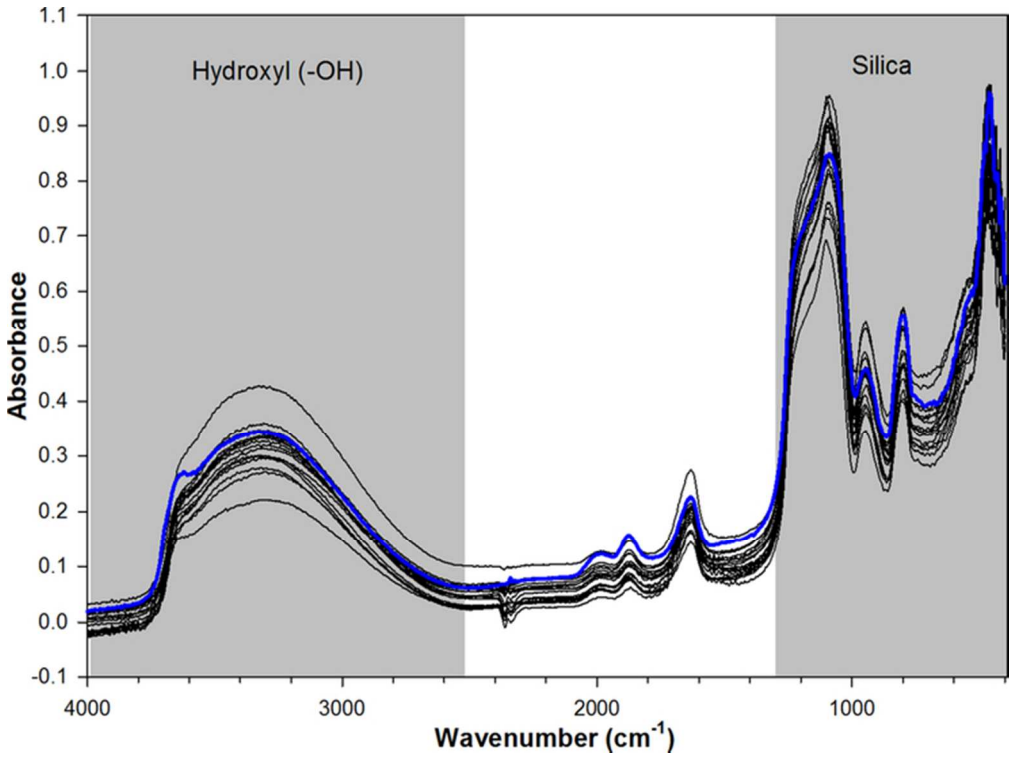

Figure 3. Fourier Transform Infrared Spectra (FTIR) of purified Heart Lake diatom samples (black) and the BFC_{mod} diatom standard (blue) composed of pure diatomite. The grey shaded areas indicate the separate hydroxyl (-OH) and silica components
62x46mm (300 x 300 DPI)

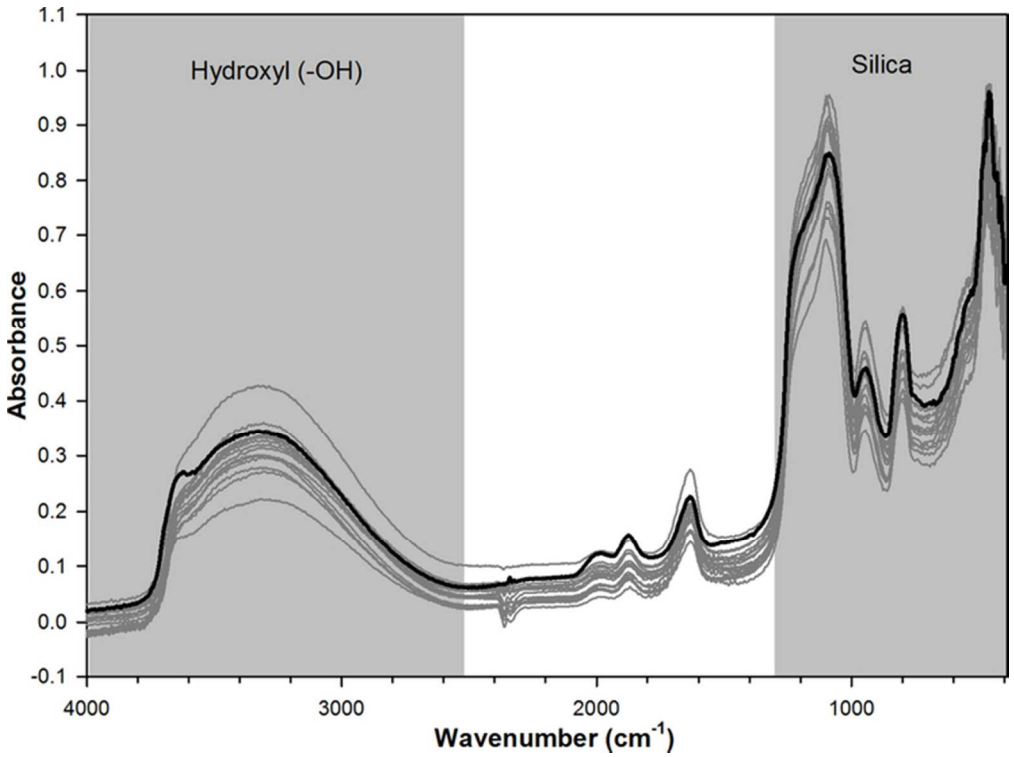

Figure 3. Fourier Transform Infrared Spectra (FTIR) of purified Heart Lake diatom samples (grey) and the BFC_{mod} diatom standard (black) composed of pure diatomite. The grey shaded areas indicate the separate hydroxyl (-OH) and silica components
62x46mm (300 x 300 DPI)

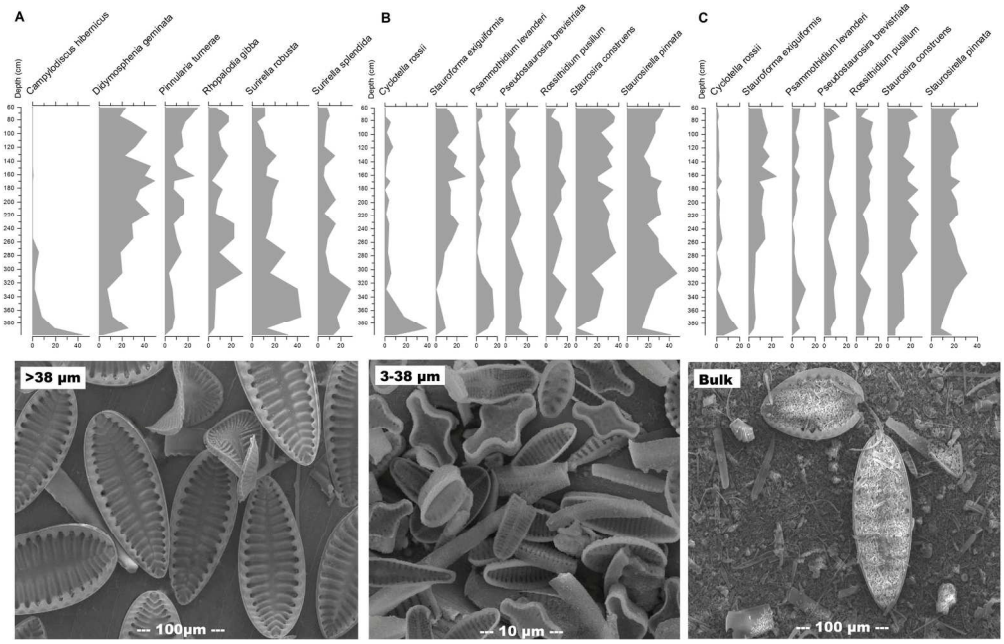

Figure 4. Stratigraphic changes in Heart Lake dominant diatom assemblages in the (A) large >38 µm (B) small 3-38 µm and (C) bulk (unprocessed) sediment diatom size fractions. Corresponding SEM images of selected diatom species are presented below each graph
111x70mm (600 x 600 DPI)

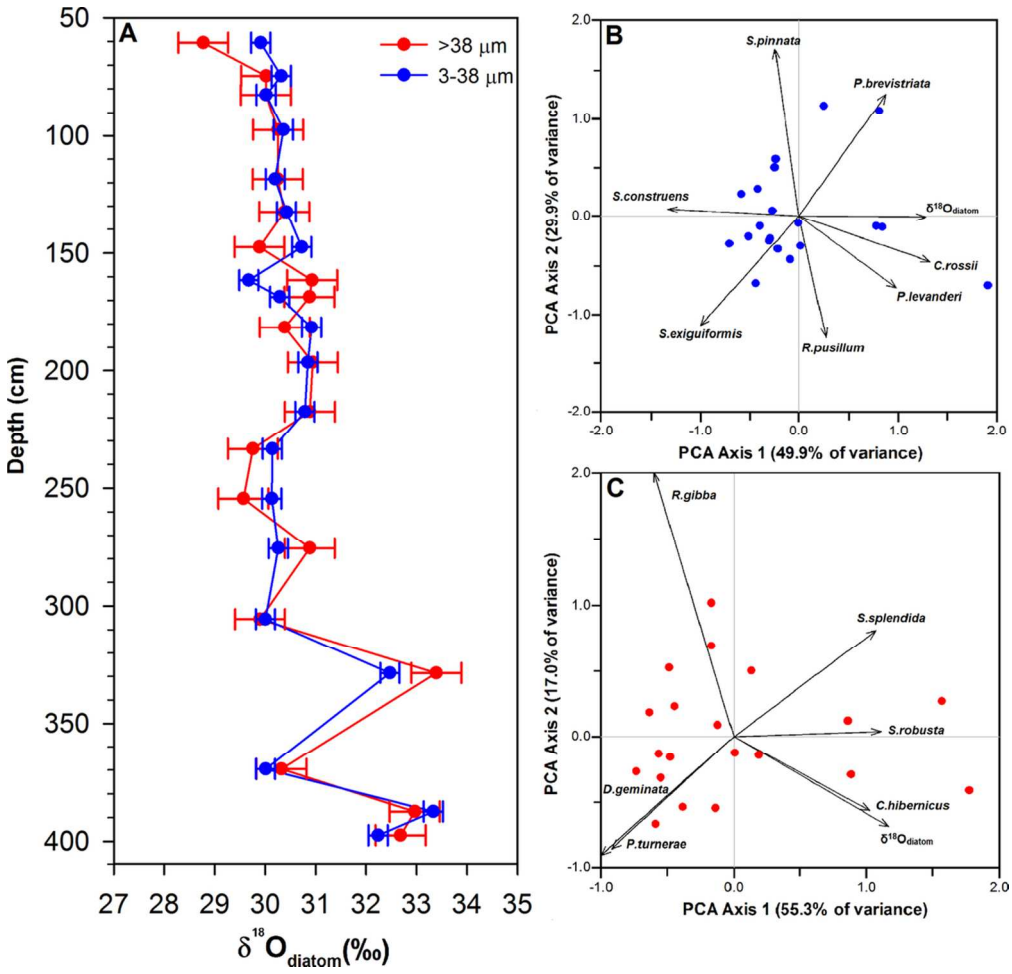

Figure 5. (A) Heart Lake $\delta^{18}O_{diatom}$ records from diatom size fractions of 3-38 µm (blue) and >38 µm (red) with analytical error. Principal components analysis of Heart Lake $\delta^{18}O_{diatom}$ and dominant diatom assemblages are displayed in the biplots showing the (B) 3-38 µm size fraction, and (C) the >38 µm size fraction
112x107mm (300 x 300 DPI)

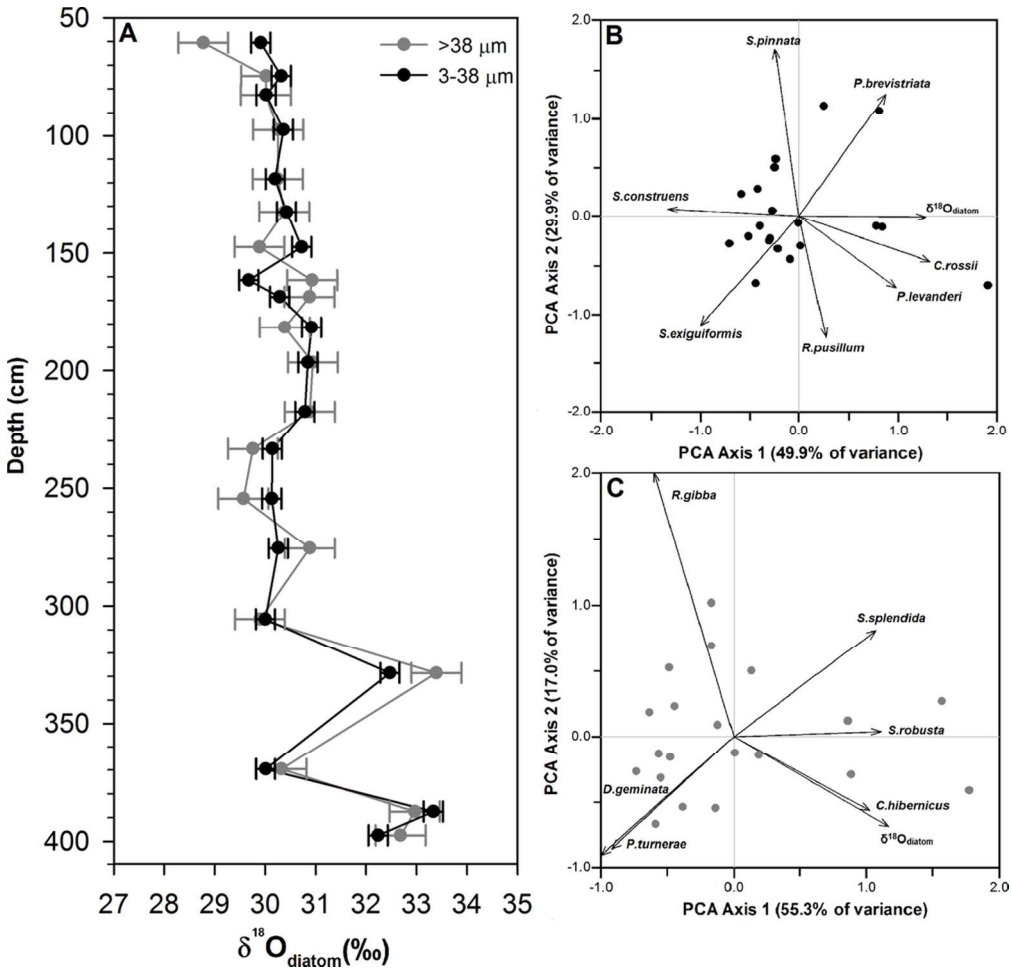

Figure 5. (A) Heart Lake $\delta^{18}O_{diatom}$ records from diatom size fractions of 3-38 µm (black) and >38 µm (grey) with analytical error. Principal components analysis of Heart Lake $\delta^{18}O_{diatom}$ and dominant diatom assemblages are displayed in the biplots showing the (B) 3-38 µm size fraction, and (C) the >38 µm size fraction
112x107mm (300 x 300 DPI)

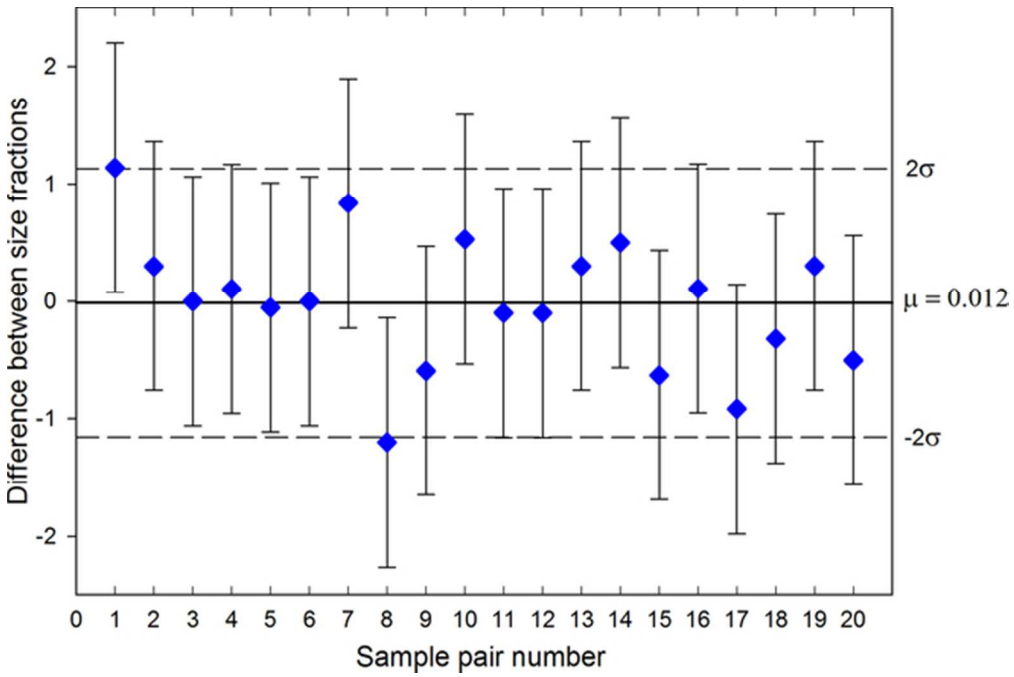

Figure 6. Difference in $\delta^{18}O_{diatom}$ between 20 pairs of different diatom size fractions from Heart Lake. Solid line indicates the mean difference between the two data sets, dashed lines represent the 2σ uncertainty range of the technique used
55x36mm (300 x 300 DPI)

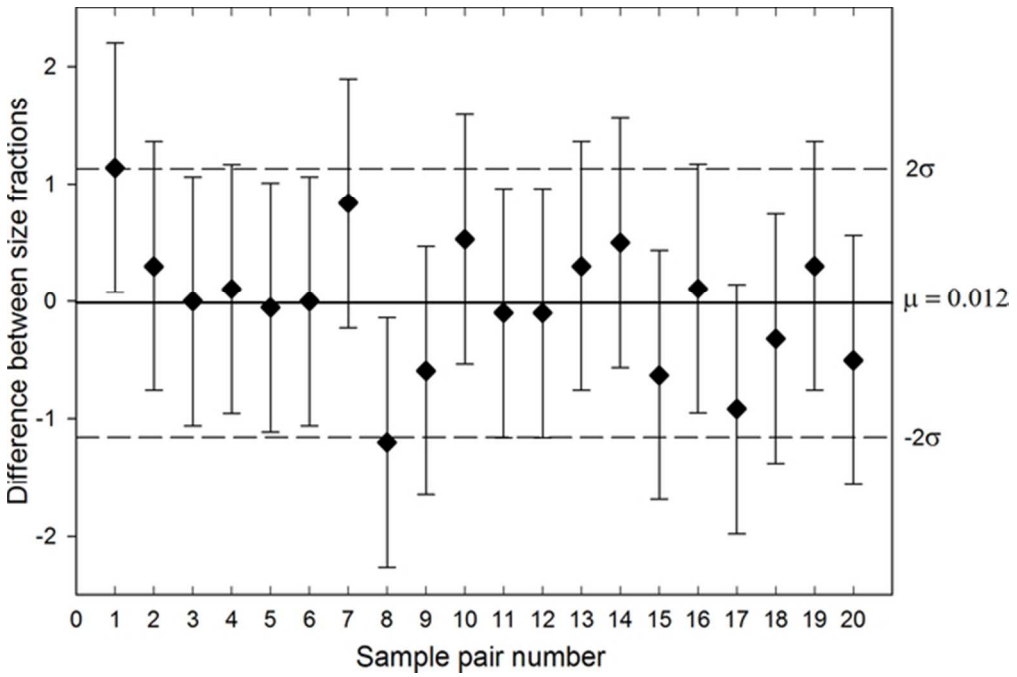

Figure 6. Difference in $\delta^{18}O_{diatom}$ between 20 pairs of different diatom size fractions from Heart Lake. Solid line indicates the mean difference between the two data sets, dashed lines represent the 2σ uncertainty range of the technique used
55x36mm (300 x 300 DPI)